



**HAL**  
open science

# Immuno-capture of biomolecules on functionalized magnetic beads: from characterization to fluorescent detection of a biomarker for Alzheimer's disease toward high performance biosensing

Ngoc van Thanh Nguyen, Claire Smadja, Myriam Taverna, Trong Khoa Mai, Frédéric Halgand, Thanh Duc Mai

## ► To cite this version:

Ngoc van Thanh Nguyen, Claire Smadja, Myriam Taverna, Trong Khoa Mai, Frédéric Halgand, et al.. Immuno-capture of biomolecules on functionalized magnetic beads: from characterization to fluorescent detection of a biomarker for Alzheimer's disease toward high performance biosensing. *Talanta*, 2023, 8, 10.1016/j.talo.2023.100264 . hal-04273225

**HAL Id: hal-04273225**

**<https://hal.science/hal-04273225>**

Submitted on 7 Nov 2023

**HAL** is a multi-disciplinary open access archive for the deposit and dissemination of scientific research documents, whether they are published or not. The documents may come from teaching and research institutions in France or abroad, or from public or private research centers.

L'archive ouverte pluridisciplinaire **HAL**, est destinée au dépôt et à la diffusion de documents scientifiques de niveau recherche, publiés ou non, émanant des établissements d'enseignement et de recherche français ou étrangers, des laboratoires publics ou privés.

1 **Immuno-capture of biomolecules on functionalized magnetic beads: from**  
2 **characterization to fluorescent detection of a biomarker for Alzheimer's disease toward**  
3 **high performance biosensing**

4

5

6 **Ngoc Van Thanh Nguyen<sup>1,2</sup>, Claire Smadja<sup>1\*</sup>, Myriam Taverna<sup>1</sup>, Trong Khoa Mai<sup>3</sup>,**  
7 **Frédéric Halgand<sup>4</sup>, Thanh Duc Mai<sup>1\*</sup>**

8 <sup>1</sup> *Université Paris-Saclay, CNRS, Institut Galien Paris-Saclay, 91400, Orsay, France.*

9 <sup>2</sup> *Faculty of Pharmacy, HUTECH University, Ho Chi Minh city, Vietnam*

10 <sup>3</sup> *Department of Oncology and Nuclear Medicine, University of Medicine and Pharmacy, Hanoi*  
11 *National University*

12 <sup>4</sup> *Université Paris Saclay-CNRS, Institut de Chimie Physique, 91400, Orsay, France*

13

14

15

16 **Correspondence:**

17 E-mail: [claire.smadja@universite-paris-saclay.fr](mailto:claire.smadja@universite-paris-saclay.fr); Fax: +33-1-46-83-55-51

18 [thanh-duc.mai@universite-paris-saclay.fr](mailto:thanh-duc.mai@universite-paris-saclay.fr)

19

20 **Keywords:** magnetic beads, density and orientation, antibody anti- amyloid beta, size exclusive  
21 chromatogram, enzyme digestion, IdeZ.

22

23

24

25

26 **Abstract**

27 It is reported herein a new approach to study the orientation and density of mouse antibody  
28 grafting on magnetic beads, serving for immunoassays and biosensors with fluorescent  
29 detection of biomolecules. This approach is based on selective enzymatic digestion of target  
30 grafted antibodies at a specific site below the hinge position to provide F(ab')<sub>2</sub> and Fc  
31 fragments, followed by separation and determination of these fragments with size exclusion  
32 chromatography (SEC) coupled with fluorescence detection (FLD). The developed method was  
33 applied for evaluation of immunoglobulin (IgG2a) grafting capacity on three different  
34 biofunctionalized magnetic beads (i.e., Tosyl-activated, carboxylic, protein G). Tosyl-activated  
35 and protein G beads at different optimal grafting IgG: bead ratios (i.e., 110 µg: 1000 µg and 240  
36 µg: 1000 µg, respectively) exhibited superior grafting capacity than carboxylic counterparts.  
37 Under the optimized conditions, more than 70 % of antibodies were grafted on tosyl-activated  
38 and protein G beads in the right orientation. This approach was then demonstrated with different  
39 commercially available antibodies specific to amyloid-beta peptide 1-42 (Aβ<sub>1-42</sub>) for magneto-  
40 immunoassays and fluorescent detection of this peptide that is an established biomarker for  
41 molecular diagnosis of Alzheimer's disease.

42

43

44

45

46

47

48

49

50

51 **1. Introduction**

52 Immuno-enrichment and immunoassays, relying on the capture of target peptides and proteins  
53 via specific antibodies for their subsequent preconcentration and fluorescent detection, are the  
54 gold techniques used in bioanalysis and biosensing. Among all solid supports for such  
55 purpose, magnetic beads have gained great attention thanks to the ease of manipulation via an  
56 external magnetic field and a variety of functionalities (commercially) available for magnetic  
57 particles [1, 2]. The performance of immunocapture on magnetic beads nevertheless depends  
58 significantly on density and orientation of the grafted antibodies in order to allow their  
59 efficient and selective interaction with target molecules as well as avoid / minimize non-  
60 specific adsorption [3-5]. Control and characterization of on-beads immobilized antibodies  
61 are therefore of utmost importance to achieve the best immunocapture and immunoassay  
62 performance. Different characterization strategies have been developed for such purpose,  
63 notably spectrophotometric and colorimetric assays [6, 7]. Gagey-Eilstein et al.  
64 communicated a chemiluminescent test to monitor the antibody grafting rate on streptavidin-  
65 magnetic beads [8]. These methods nevertheless cannot provide any information on antibody  
66 orientation and/or can induce measurement biases mainly related to possible background  
67 interferences [9-11]. Other methods such as surface plasmon resonance (SPR), dual  
68 polarization interferometry, spectroscopic ellipsometry and atomic force microscopy, can  
69 provide insight on antibody orientation mainly by measuring antibody dimensions/thickness  
70 on surfaces or shift angle [12-17]. Indirect methods for quantification of proteins on the  
71 surface of nanoparticles (NPs) were as well proposed, relying on hydrolysis of grafted  
72 proteins, followed by spectrophotometric or chromatographic quantification of primary  
73 amines, amino acids or peptides in solution [18-20]. Our group recently proposed a new  
74 simple and rapid analytical approach to evaluate human antibody orientation and density on  
75 magnetic beads applied for immunocapture of a biomarker of inflammation (TNF- $\alpha$ ) [21].

76 This approach relies on the cleavage of immobilized antibodies by IdeS, a highly specific  
77 protease for human immunoglobulin G (hIgG). This approach using IdeS nevertheless is not  
78 adapted to mouse IgG, which represents the majority of antibodies commercially available for  
79 bioanalysis. Indeed, in the context of molecular diagnosis of Alzheimer's disease (AD), which  
80 is the most prevalent neurodegenerative disease worldwide causing a huge burden to the  
81 society and having no efficient AD treatment so far [22], mouse antibodies have been most  
82 widely used for immunoassays of amyloid (A $\beta$ ) beta peptides (notably A $\beta$  1-42 and A $\beta$  1-40  
83 which are established biomarkers for AD). No human antibodies recognizing specifically  
84 these compounds have been available so far.

85  
86 From this rationality, we report in this study the development of an analytical approach to  
87 simultaneously characterize the density and orientation of grafted mouse antibody on  
88 magnetic beads. This approach relies on selective enzymatic digestion of immobilized mouse  
89 antibodies at one specific site below the hinge region using FabRICATOR Z (IdeZ) to give  
90 F(ab')<sub>2</sub> and Fc fragments from mouse antibodies, followed by separation and determination  
91 of these fragments with size exclusion chromatography (SEC) coupled to fluorescent  
92 detection (FLD). Optimization of the SEC-FLD method was made to allow separation of the  
93 F(ab')<sub>2</sub> and Fc fragments from residual antibodies and the enzyme, allowing non-bias  
94 determination of the digestion efficiency via the F(ab')<sub>2</sub> / Fc ratios. The developed approach  
95 was applied for three functionalized magnetic beads (i.e., Tosyl-activated, carboxylic, Pierce  
96 Protein G) grafting with immunoglobulin (IgG2a) from mouse. Following the antibody-  
97 grafting optimizations that can be monitored with our method, the activity of grafted  
98 antibodies was confirmed via on-bead immunoassays with fluorescent detection of amyloid  
99 beta 1-42 peptide (A $\beta$ <sub>1-42</sub>) that is an established biomarker for AD molecular. The work was  
100 extended to three antibodies specific to different epitopes of A $\beta$ <sub>1-42</sub> (i.e., NAB228 for N-

101 terminal, 12F4 for C-terminal, and 4G8 for 17-24 epitopes), serving for evaluation of the  
102 performance of bead-based immunoassays of A $\beta$ <sub>1-42</sub>.

103

## 104 **2. Experimental**

### 105 ***2.1. Chemicals, reagents and samples***

106 2-(Cyclohexylamino)ethanesulfonic acid (CHES), Tris(hydroxymethyl)aminomethane  
107 (TRIS), sodium dodecyl sulphate (SDS), sodium hydroxide (NaOH), potassium hydroxide  
108 (KCl), acid boric (H<sub>3</sub>BO<sub>3</sub>), sodium dihydrophosphate (NaH<sub>2</sub>PO<sub>4</sub>), disodium hydrophosphate  
109 (Na<sub>2</sub>HPO<sub>4</sub>), Tween 20, ammonium sulfate ((NH<sub>4</sub>)<sub>2</sub>SO<sub>4</sub>), EDC (N-(3-Dimethylaminopropyl)-  
110 N'-ethylcarbodiimide hydrochloride), S-NHS (N-Hydroxysulfosuccinimide sodium salt),  
111 mouse IgG2a (2 mg/ml) (mIgG), phosphate buffer saline 10X (PBS), Tris buffer saline 10X  
112 (TBS), ammonium hydroxide (NH<sub>4</sub>OH), human IgG from whole serum (hIgG at 10 mg/ml),  
113 as well as different anti-Alzheimer antibodies (1 mg/ml), including NAB228 and 6E10-HRP  
114 were all provided by Sigma Aldrich (St. Louis, MO, United States). Other antibodies 12F4-  
115 HRP, 12F4, and 4G8 were obtained from Biologend (San Diego, California, United State).  
116 HPLC grade isopropanol (IPA), methanol and acetonitrile were purchased from VWR  
117 (Pennsylvania, US). FabRICATOR enzyme (Ides) and FabRICATOR Z enzyme (Idez) were  
118 obtained from Genovis (Lund, Sweden). Amyloid beta peptide Ab 1-42 (A $\beta$ <sub>1-42</sub>) was  
119 purchased from Eurogentec (Seraing, Belgium). FP-488 NHS ester solution was purchased  
120 from Interchim (Montluçon, France). Pierce Protein G (ProG), Tosyl-activated (Ts) and  
121 Carboxylated (COOH) magnetic beads, QuantaRed Enhanced Chemifluorescent HRP kit  
122 were provided by Thermo Fisher (Massachusetts, United States). All buffers were prepared  
123 with deionized water and were filtered through a 0.22  $\mu$ m membranes (Pall Corporation, New  
124 York, USA) prior to use. For mass spectrometry experiments, acetonitrile and formic acid  
125 were purchase from Sigma Aldrich.

126

## 127 **2.2. Apparatus and Material**

128 Deionized water used in all experiments was purified using a Direct-Q3 UV purification system  
129 (Millipore, Milford, MA, USA). Conductivity and pH values of buffer solutions and samples  
130 were measured by a Seven Compact pH meter (Mettler Toledo, Schwerzenbach, Switzerland).  
131 SEC-FID experiments were carried out using a 1260 Agilent UPLC, and a 1260 fluorescent  
132 detector ( $\lambda_{\text{excitation}}$ : 280 nm,  $\lambda_{\text{emission}}$ : 345 nm) (Agilent Technologies, Santa Clara, CA, USA).  
133 Two columns, including Agilent AdvanceBio SEC (2.7 $\mu$ m particle size, 130A° pore size, i.d  
134 7.8 , length 300 mm) and BioSEC-3 (3 $\mu$ m particle size, 300A° pore size, i.d 4,6 mm, length  
135 300 mm) were employed for SEC-FLD at temperature of 25 °C. Fluorescence detection with  
136 the excitation and emission wavelengths of 530 nm and 582 nm respectively were carried out  
137 with a FP-750 Spectrofluorometer from Jasco (Lisses, France) using a 40  $\mu$ L quartz cuvette  
138 (Starna Scientific, Essex, England). Mass spectrometry measurements were performed on a  
139 QToF Synapt G2 Si (Waters, Manchester) equipped with ion mobility. Parameters were  
140 optimized to obtain the best signal. In brief, capillary voltage was set to 3.5 kV, source  
141 temperature to 40°C, the cone voltage and the offset were fixed at 50 V, désolvation  
142 temperature was 450 °C, and nebulizer gas flow to 500 L/hr. Calibration was performed on the  
143 500 to 5000  $m/z$  range using TFANa. Error on the measurement was 0.2 ppm.

144

## 145 **2.3. Methods**

### 146 **2.3.1. Antibody digestion in solution**

147 IdeS FabRICATOR enzyme 5000 U and IdeZ FabRICATOR Z enzyme 2000 U were  
148 dissolved in 100  $\mu$ L and 50  $\mu$ L miliQ water, respectively, then aliquoted to 2  $\mu$ L and stored at  
149 -20°C. For IgG digestion, 2  $\mu$ L IdeS enzyme (100UI) was mixed with 50  $\mu$ L of 100 mM  
150 phosphate buffer (pH 7.0) whereas 2  $\mu$ L IdeZ enzyme (80UI) was added to 50  $\mu$ L of 10mM

151 phosphate buffer and 10 mM sodium chloride (pH 6.5). hIgG and 6E10 were diluted in PBS  
152 to 50  $\mu$ L at concentration of 0,1 mg/ml and then digested with IdeS at 37<sup>0</sup>C on a thermo-  
153 mixer at 650 rounds per minute (rpm) for 90 minutes. NAB228 and 6E10 (0,1 mg/ml) were  
154 prepared and digested with IdeZ under the same conditions for 120 minutes.

155

### 156 **2.3.2. Antibody grafting on magnetic beads**

#### 157 *Protein G magnetic bead*

158 50  $\mu$ L of ProG magnetic beads (10 mg/mL) was added to 2 mL LoBind Eppendorf vials and  
159 gently vortexed with 500  $\mu$ L of Tris solution containing 0.05 % v/v of Tween 20. The  
160 supernatant was removed, and the beads were washed one more time with 1 mL of Tris-  
161 Tween 20 (0.05%). A magnet was employed to retain magnetic beads during removal or  
162 addition of a suspension solution. After removal of the supernatant, a predefined volume (0-5-  
163 15-22,5-45-60-75-90  $\mu$ L) of NAB228 at 2 mg/mL was subsequently added to beads. The Tris-  
164 Tween 20 (0.05%) solution was then added to 500  $\mu$ L. The mixtures were then incubated at  
165 25<sup>o</sup>C, 650 rpm for 1 hour on a Thermomixer. The protocol was also carried out with 100  $\mu$ L  
166 ProG (10 mg/mL) and 4 batches of NAB228 (0-10-55-120  $\mu$ L at 2 mg/mL). After incubation,  
167 the supernatants were collected. The beads were then washed twice with 500  $\mu$ L of Tris-  
168 Tween 20 (0.05%) solution. The washing solutions were collected for subsequent analyses.

169

#### 170 *Tosyl-activated magnetic bead*

171 10  $\mu$ L of Dynabeads MyOne Tosylactivated (100 mg/mL) was added to 2mL LoBind  
172 Eppendorf vials and washed with 500 $\mu$ L of 0.1 M sodium borate buffer (pH 9.5) using a  
173 Thermomixer for 15 min C at 25<sup>o</sup>C and 650 rpm. Pre-defined volumes (0-10-55-90-120  $\mu$ L)  
174 of NAB228 solution (2 mg/mL) were added to beads. 60  $\mu$ L of 3M ammonium sulphate  
175 buffer (pH 9.5) and 20  $\mu$ L of 0.1M sodium borate buffer were then added. The mixtures were

176 then incubated at 37 °C on a Thermomixer (650 rpm) for 16h. The supernatants were  
177 collected with the help of a magnet. The beads were washed twice with 500 µL of PBS-  
178 Tween 20 (0.05%) and once with 500 µL of PBS. The washing solutions were also collected  
179 for subsequent analyses by SEC-FLD.

180

#### 181 *Carboxylated magnetic bead*

182 100 µL of a Dynabeads MyOne carboxylic acid suspension (10 mg / mL) were rinsed twice  
183 with 1 mL PBS after removing the suspending solution. 500 µL of EDC solution (10 mg / mL  
184 inPBS) and 500 µL of S-NHS solution (10 mg / mL in PBS 1X) were then added into the  
185 washed beads, followed by the addition of NAB228 2 mg/ml (10 µL or 55 µL). The mixture  
186 was incubated for 3 hours under 650 rpm at room temperature (RT). The supernatant was  
187 collected. The antibody-bound magnetic beads were subsequently washed twice with 1 mL of  
188 PBS, followed by an incubation at RT with 1mL of 50 mM Tris-HCl (pH 7.4) for 15 min in  
189 order to quench the non-reacted activated carboxylic acid groups. The antibody-bound  
190 magnetic beads were then washed 3 times with 1 mL of PBS - 0.1 % Tween-20. A magnet  
191 was employed to retain magnetic beads during removal or addition of a suspension solution.

192

#### 193 **2.3.3. Digestion of NAB228 grafted on magnetic beads by IdeZ**

194 100 µL of enzyme Idez (3 UI) was used for 1 µg NAB228. The enzyme solutions were added  
195 directly to grafted and washed magnetic beads and incubated for 3h at 37 °C on a  
196 Thermomixer at 650 rpm. Further optimization of the enzymatic digestion procedure can be  
197 referred to section 3.1.

198

#### 199 **2.3.4. SEC-FLD conditions**

200 The SEC-FLD analyses of digested samples were conducted on two Agilent columns:  
201 BioSEC-3 (3 $\mu$ m particle size, 300 $\text{\AA}$ , i.d 4,6 mm, length 300 mm) and AdvanceBio SEC  
202 (2.7 $\mu$ m particle size, 130 $\text{\AA}$  pore size, i.d 7.8, length 300 mm). Both columns were  
203 equilibrated with the mobile phase for 5 column volumes prior to analysis; and flushed with a  
204 mixture of miliQ water (80%) and MeOH (20%) for 15 column volumes after each analysis.  
205 The flow rate was fixed at 0,3 ml/min for both columns. For each analysis, 2  $\mu$ L of sample  
206 was injected, and analyzed with the phosphate buffer 50 mM that contains 10 % IPA and 150  
207 mM KCl (pH 6,8).

208

209 Calibration curves were made using native NAB228 prepared in different matrices and under  
210 different conditions that were used for on-bead antibody grafting protocols. The calibration  
211 curve served for the study on Tosyl-activated beads was made with NAB228 (at six points  
212 from 0,05 to 0.3  $\mu$ g) diluted in ammonium sulphate 3 M and sodium borate buffer 0,1 M at  
213 pH 9.5 and incubated on Thermomixer at 37 $^{\circ}$ C during 16h. The one used for the study on  
214 proG beads was done with NAB228 (6 concentration points) prepared in Tris-Tween 20  
215 (0.05%) and incubated at 25 $^{\circ}$ C for 1h on Thermomixer. The non-grafted condition was used  
216 as the reference with six points of native mouse IgG2a prepared in PBS. Three SEC-FLD  
217 analyses were implemented for each concentration. The respective calibration curve for each  
218 bead type was used to determine the non-grafted NAB228 amount in supernatant and washing  
219 solutions. The successfully grafted NAB228 was estimated from the difference between the  
220 initial antibody concentration and the recovered ones in the supernatant and washing  
221 solutions.

222

223 ***2.3.5. Immunoassay of A $\beta$  1-42 peptide***

224 A volume of 50  $\mu$ L A $\beta$  1-42 was incubated with 200  $\mu$ g magnetic beads coated with the desired  
225 antibodies (12F4, 4G8 or NAB228) and 5  $\mu$ L 6E10- HRP or 12F4- HRP antibodies at  
226 concentration of 0.04  $\mu$ g/ml in PBS 1X on a mixer at RT for 1 hour. The beads were then  
227 washed 3 times (10 min each time on a mixer) with 400  $\mu$ L PBS 1X/ 0.1 % BSA (m/v)/ 0.1 %  
228 Tween- 20 (v/v). Then, 100  $\mu$ L QuantaRed solution was added to the washed beads. The  
229 incubation was carried out over 7 min on shaking, followed by addition of 10  $\mu$ L QuantaRed  
230 Stop solution. The colour intensity of the achieved solution was measured with the excitation  
231 and emission wavelengths of 530 nm and 582 nm, respectively.

232

### 233 ***2.3.6. MS measurements of A $\beta$ 1-42 peptide***

234 Five lots of A $\beta$  1-42 peptide stock solution at 2 mg/ml were prepared by balancing and  
235 dissolving in corresponding volume of DMSO. The Eppendorf vials were vortexed gently with  
236 hand. Then, the stock solutions were diluted in NH<sub>4</sub>OH 0.16% to obtain the samples at a  
237 concentration of 5  $\mu$ M. These samples were injected directly into MS to verify the quality of  
238 A $\beta$  1-42. For MS conditions see the section 2.2 above.

239

## 240 **3. Results and Discussion**

### 241 **3.1. Enzymatic digestion of grafted antibodies and analysis of released fragments**

242 Our approach (see Fig.1) to characterize the performance of on-bead antibody grafting relies  
243 on the selective enzymatic digestion of the grafted antibody below the hinge position to  
244 release (Fab')<sub>2</sub> and Fc fragments. The analysis of the remaining antibody as well as these  
245 released fragments, which are typical for an antibody, can then provide insight in the density  
246 and the orientation of the grafted antibodies thanks to the ratio of F(ab')<sub>2</sub> 's signal to Fc one.  
247 Unlike chemically mediated or trypsin-based methods, our approach is softer and more  
248 selective, and can provide both information on antibody density and orientation. The

249 challenges here were to find an appropriate enzyme that works on the target mouse antibodies  
250 and develop the subsequent separation strategy for determination of the resulting fragments.  
251 In our case, SEC which is frequently used for separation of proteins and peptides was chosen  
252 for analysis of F(ab')<sub>2</sub> and Fc fragments. The obtained F(ab')<sub>2</sub> and Fc fragments and residue  
253 IgG possess respective molecular weights of about 100, 50 and 150 kDa. Phase mobile  
254 optimization was first carried out to separate these target fragments from the residual  
255 antibodies in the solution (Fig. 2). Among two salts commonly used in SEC buffers, KCl  
256 offered more symmetric and less tailing peaks than NaCl (Fig 2 A-B vs Fig 2 C-D). Indeed,  
257 KCl was found stronger than NaCl in suppression of the secondary interaction between target  
258 molecules and the stationary phase, probably due to the larger size and higher interactivity of  
259 K<sup>+</sup> cation [23]. It was observed from Fig 2 C vs Fig. 2 D that the column of a smaller pore  
260 size (130A<sup>o</sup>) provides better resolution for separation of F(ab')<sub>2</sub> and Fc. Moreover, thanks to  
261 these optimized conditions, the peak of IdeZ enzyme was well separated from the Fc fragment  
262 (see Figs. 3 and 4), which was not the case in the previous work using IdeS [21]. This would  
263 help avoid the bias in quantification of the digested fragments.

264

265 The optimized SEC-FLD conditions were then used to monitor the IgG digestion  
266 optimization. FabRICATOR IdeS, which was found to offer fast reaction on hIgG, and was  
267 found to work well in our previous work on hIgG [21] was tested as the reference. By  
268 comparing the peak of IgG before and after digestion in Figs. 3A-B, one can see that almost  
269 80% of hIgG was digested with IdeS without optimization, whereas only 10% of mouse IgG1  
270 could be digested under the same conditions. Indeed, IdeS can digest only antibodies having  
271 CPPCPPELLG/GPSVF sequence at hinge position that is typical for human, rabbit and  
272 sheep IgG. This enzyme nevertheless is less favorable for mouse IgG, which represents the  
273 majority of antibodies commercially available for bioanalysis and is the most widely used one

274 for immunoassays of A $\beta$  peptides. To overcome this problem, FabRICATOR Z IdeZ was  
275 selected for mouse IgG. This kind of enzyme shows its specificity on mouse IgG2a or IgG3,  
276 having CPAPNLLG/ GPSVF sequence at the hinge site. As can be seen in Fig 3C, more than  
277 60% of NAB228 antibody (mouse IgG2a type) was digested in the first trial, which provided  
278 encouraging results. IdeZ enzyme was therefore chosen for further optimization of mouse  
279 IgG2a digestion. A two-level-three-factors ( $3^2$ )  $\frac{1}{2}$  fraction experiment was designed to  
280 optimize the digestion protocol using Minitab statistical software 17. The three factors  
281 covered (i) enzyme unit for 1  $\mu$ g IgG digestion (1 - 3 UI), (ii) incubation time (2 to 4 hour) and  
282 (iii) temperature (low 30°C and high 44°C). The response to be evaluated was the digestion  
283 efficiency estimated via F(ab')<sub>2</sub> : Fc peak-area-ratio. A Pareto chart was used to determine the  
284 optimal conditions for complete digestion of IgG while using the lowest enzyme unit as  
285 possible. Among the investigated factors, the one with the highest impact was found for the  
286 added enzyme unit. As can be seen from Fig. 4, with 3 U of enzyme IdeZ for 1  $\mu$ g IgG (in an  
287 incubation over 3 hours at RT), quasi-complete digestion (98%) of IgG in solution, calculated  
288 according to peak areas of initial IgG and residual one after digestion, could be achieved.  
289 Compared to the digestion performance obtained with the commercial protocol for IdeZ (see  
290 Figs. 2 C-D where there was much residual IgG after the digestion), that achieved with our  
291 optimized conditions is superior with almost no trace of IgG left (Fig. 4).

292

### 293 **3.2. Optimization of the density and orientation of antibodies grafted on magnetic beads**

294 The optimized digestion conditions (i.e., incubation with 3 UI IdeZ over 3h at 37 °C) and the  
295 optimized SEC-FLD ones (i.e., column of 130 Å pore-size, phosphate buffer containing 150  
296 mM KCl) were employed to release and determine the F(ab')<sub>2</sub> and Fc fragments from on-  
297 bead grafted NAB228 antibody (mouse IgG). Quantification of grafted NAB228 was made  
298 with following the formula (1), respectively:

299 
$$m_{\text{grafted}} = m_{\text{initial}} - (m_{\text{supernatant}} + m_{\text{washing}}) \quad (1)$$

300 *where*

301 *m<sub>initial</sub>, m<sub>grafted</sub>, m<sub>supernatant</sub> and m<sub>washing</sub> are the initial quantity of antibodies, the*  
302 *quantity of antibodies grafted on 1000 µg beads, and those of remaining antibodies in*  
303 *the supernatant and washing solutions, respectively.*

304

305 The peak ratios for F(ab')<sub>2</sub>/Fc fragments released from NAB228 antibodies grafted on Tosyl-  
306 activated, ProG and carboxylated magnetic beads were determined and compared (Fig. 5).

307 With the same quantity of antibodies available for grafting, proG and tosyl-activated beads  
308 allowed higher amount of grafted NAB228, whereas very little trace of grafted antibodies  
309 could be found with carboxylated ones. As shown in Fig 5A and B, proG and tosyl-activated  
310 beads would require different initial antibody amount to achieve the best F(ab')<sub>2</sub>/ Fc ratio.

311 The best grafted antibody density and orientation was achieved with 110 µg antibodies per 1  
312 mg bead for tosyl-activated beads (at F(ab') / Fc of 2.9), whereas for proG beads the best  
313 F(ab')<sub>2</sub> / Fc ratio of 2.5 was achieved at a higher quantity of 240 µg antibodies per 1 mg  
314 beads (Fig. 5C). This can be explained by the fact that tosyl-activated beads with a covalent  
315 group (H<sub>3</sub>CC<sub>6</sub>H<sub>4</sub>SO<sub>2</sub>) has more affinity to Fc fragment. Note that further addition of  
316 antibodies led to less grafting performance on tosyl-activated beads (Fig. 5C), probably due  
317 the abundant presence of PBS used for antibody suspension, which is the blocking solution  
318 and not favorable for tosylated groups on magnetic beads, according to the instructions in the  
319 commercial protocol. In the case of proG, at low IgG quantity (< 50 µg), the non-covalent  
320 linkage is more effective towards F(ab')<sub>2</sub>, leading to less-oriented antibody grafting (with  
321 decreased F(ab')<sub>2</sub> / Fc peak ratio). At higher IgG quantity, the tendency was reversed, leading  
322 to an improved in F(ab')<sub>2</sub>/Fc peak ratio for ProG beads. This important observation indicates  
323 that different magnetic beads would require different antibody quantities to reach the

324 maximum density and best orientation. Under our best grafting conditions, 74.4 % of  
325 antibodies grafted on tosyl-activated beads were at the right orientation, calculated from the  
326  $(F(ab')_2 / (Fc + F(ab')_2))$  peak ratio. This was 71.9 % for the case of ProG beads. Using the  
327 formula (1), the maximum grafted quantity of NAB228 antibodies on ProG and tosyl-  
328 activated beads were estimated to be 43  $\mu$ g and 35  $\mu$ g per 1000  $\mu$ g beads, respectively. Note  
329 that different conditions (i.e., the matrices, the temperatures and incubation times) were used  
330 for grafting antibodies on different beads. To avoid bias in the quantification of grafted  
331 antibodies, different calibration curves were made for different bead types, using NAB228  
332 prepared in respective grafting matrices (see Fig. S1 in the supporting information ESI). Note  
333 also that the peak of IdeZ was observed together with those of  $F(ab')_2$  and Fc fragments after  
334 the digestion (Fig. 5). The peaks of IdeZ in the supernatants after incubation with different  
335 beads were lower than that of IdeZ in the initial one, which was due to some absorption of  
336 IdeZ on to ProG and tosyl-activated beads during the incubation for digestion of grafted IgG,  
337 as demonstrated in Fig. S2 in the ESI. The peak of residual IdeZ, if not well separated from  
338 those of target  $F(ab')_2$  and Fc, could induce some interference to these target peaks, and  
339 therefore confirm again the need to have an improved SEC-FLD method in our case to  
340 separate IdeZ from the target fragments.

341

### 342 **3.3. Immunoassays with fluorescent detection of A $\beta$ 1-42 on magnetic beads**

343 To validate the aforementioned optimization, the tosyl-activated and proG beads grafted with  
344 NAB228 (an anti A $\beta$ 1-42 antibody specific at N-terminal of this peptide) at their optimal  
345 concentrations were employed to carry out immunoassays of A $\beta$ 1-42 (Fig. 6). Since A $\beta$ 1-42  
346 peptide is prone to aggregation [22], the good quality of each batch was first confirmed with  
347 MS (see Fig. S3 in the ESI). A $\beta$ 1-42 solutions were prepared freshly from the confirmed  
348 batch just before each immunoassay series. Detection in this case was made with another anti

349 A $\beta$ 1-42 antibody specific at C-terminal of this peptide, which is bound with HRP to trigger  
350 subsequently the enzymatic reaction with Quanta Red substrate followed by fluorescent  
351 detection (Fig. 6A). NAB228 grafted on ProG showed higher fluorescent signals than those  
352 obtained with tosyl-activated beads (Fig. 6B). Further results on the immunoassays of A $\beta$ 1-42  
353 can be seen in Fig. S4 in the ESI. This observation was in good accordance with the results  
354 indicating that more antibodies were grafted on ProG beads than on tosyl-activated ones, with  
355 equivalent antibody grafting orientation (see section 3.2 above).

356

357 Employing the antibody / bead ratios optimized for NAB228, the test on immunocapture of  
358 A $\beta$ 1-42 was also extended to other antibodies specific to this peptide, i.e., 12F4 specific to N-  
359 terminal and 4G8 specific to 17-24 epitopes (Fig. S5 in the ESI). An antibody specific to N-  
360 terminal of A $\beta$ 1-42 (6E10-HRP) was employed in this case for detection of the captured  
361 peptide. Among three capture antibodies, NAB228 exhibited the best on-bead capture  
362 performance, regardless of the bead type used (tosyl-activated or ProG). The signals obtained  
363 with 12F4 and 4G8 were relatively low for both types of beads. The limit of detection was 10  
364 nM for NAB228 and 20 nM for other antibodies. This implies that for each antibody, re-  
365 optimization of the antibody : bead ratio would be needed. And the optimal ratio achieved for  
366 1 specific antibody (NAB228 in our case) cannot be generic to other ones. This remark is  
367 important, because so far one tends to follow the same *antibody : bead* ratio according to the  
368 established grafting protocol for different antibodies, which may lead to non-optimal  
369 immunocapture performance.

370

#### 371 **4. Conclusions**

372 We developed successfully an enzyme-based approach for evaluation at same time the density  
373 and orientation of mouse IgG<sub>2a</sub> immobilized on three different magnetic beads. Using this

374 approach to follow the optimization of antibody grafting conditions, more than 70 % of  
375 antibodies could be grafted on tosyl-activated and protein G beads in the right orientation. The  
376 developed method was applied for monitoring the density and orientation of anti- A $\beta$  1-12  
377 antibodies on different magnetic bead supports, serving for immunoassays and fluorescent  
378 detection of this amyloid-beta peptide. The antibody NAB228 grafted on ProG beads  
379 exhibited the best performance, with the detection limit of 10 nM achieved for A $\beta$  1-12. The  
380 strategy using IdeZ enzyme to check the density and orientation of mouse antibodies on  
381 magnetic beads provides us a powerful tool for optimization and improvement of the  
382 performance of immunoassays and biosensing of target biomolecules on magnetic beads.  
383 Other biosensing applications targeting different biomarkers using this enzyme-based method  
384 are envisaged to further demonstrate the significance of our work.

385

386

### 387 **Acknowledgement**

388 This work has been financially supported by the ‘bourse d’excellence de l’ambassade de  
389 France’ (for PhD scholarship of N.V.T. Nguyen).

390

391

392

393

394

395

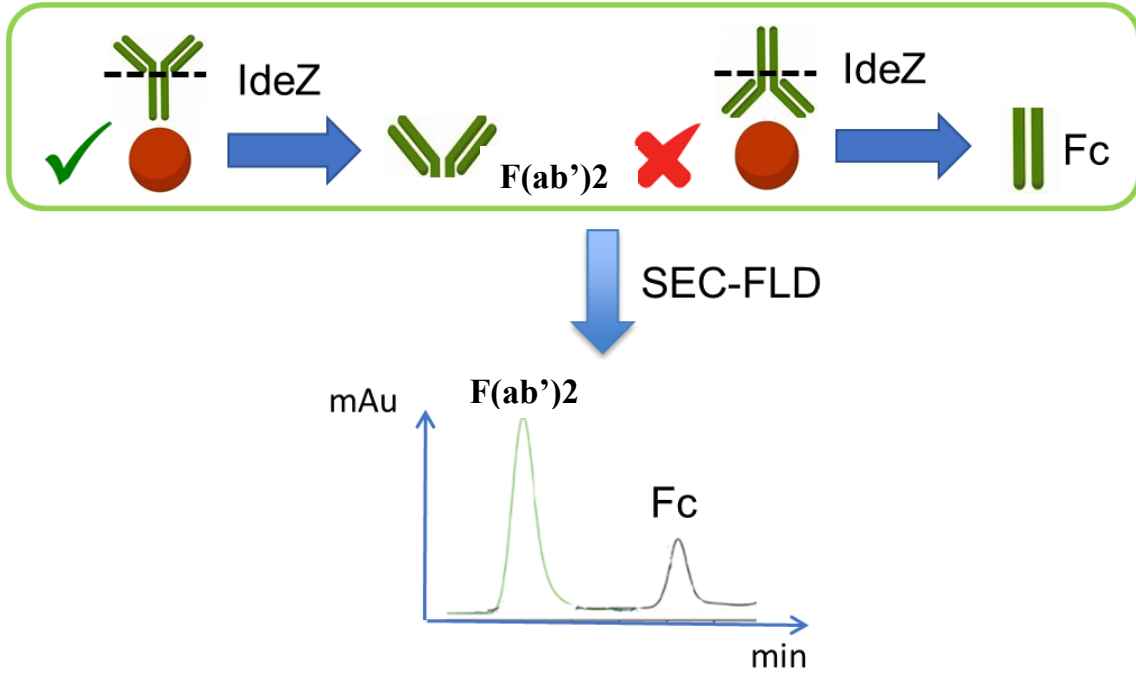
396

397

398

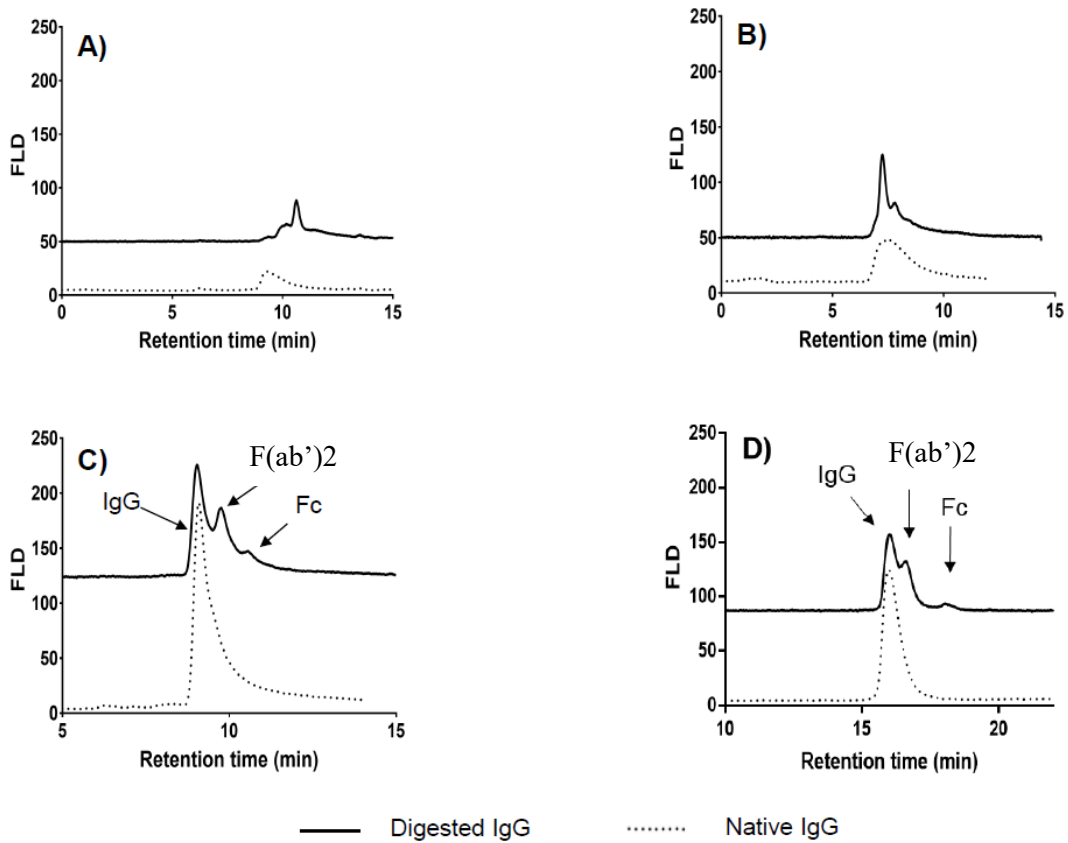
399 **Figure captions:**

400 Fig. 1. Proposed strategy for characterization of density and orientation of antibodies  
401 grafted on magnetic beads.



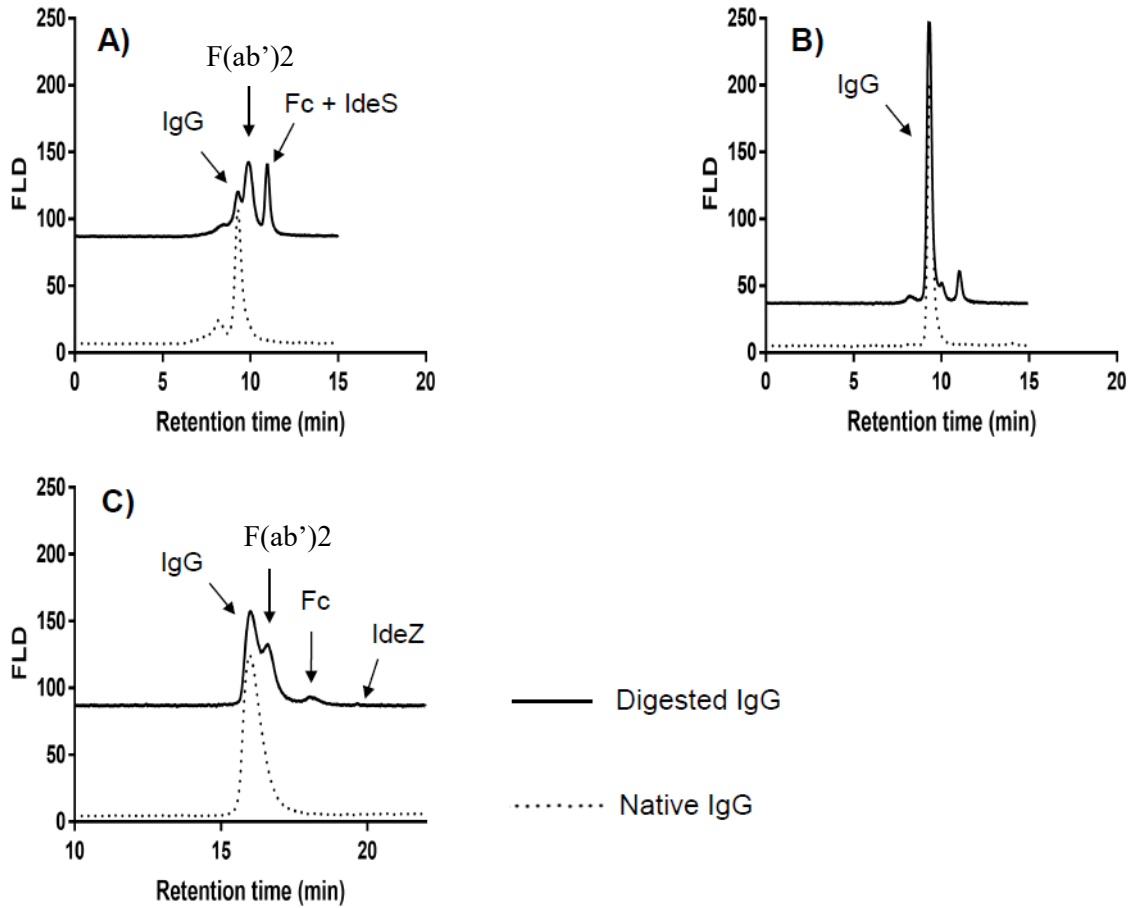
402  
403  
404  
405  
406  
407  
408  
409  
410  
411  
412  
413  
414  
415

416 Fig. 2. Analysis of IdeZ-digested NAB228 by SEC- FLD using a column having  
417 dimensions of 4.6 x 300mm, particle size of 3 $\mu$ m; pore size of 300 $\text{\AA}$  and the  
418 phosphate buffer containing A) 150 mM NaCl, C) 150 mM KCl; or a column  
419 having dimensions of 7.8 x 300mm, particle size of 2.7 $\mu$ m, pore size of 130 $\text{\AA}$  and  
420 the phosphate buffer containing B) 150 mM NaCl, and D) 150 mM KCl.



421  
422  
423  
424  
425  
426  
427  
428  
429

430 Fig. 3. Digestion of 0,1 mg/ml antibodies in PBS: A) human IgG by IdeS; B) Mouse IgG1  
431 (6E10) by IdeS; C) Mouse IgG2a (NAB228) by IdeZ. SEC- FLD conditions:  
432 column having dimensions of 7.8 x 300mm, particle size of 2.7 $\mu$ m, pore size of  
433 130Å and the phosphate buffer containing 150 mM KCl.



434

435

436

437

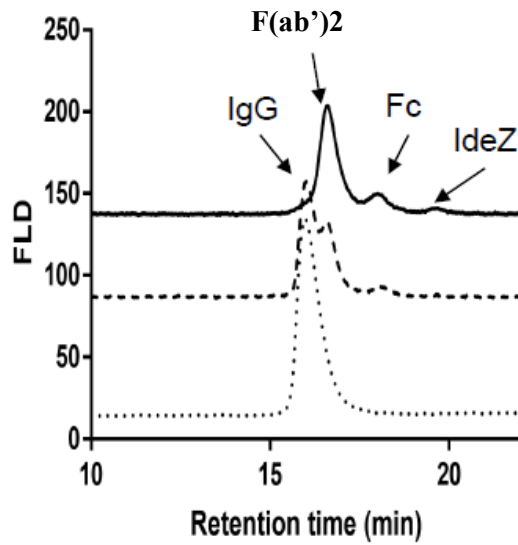
438

439

440

441

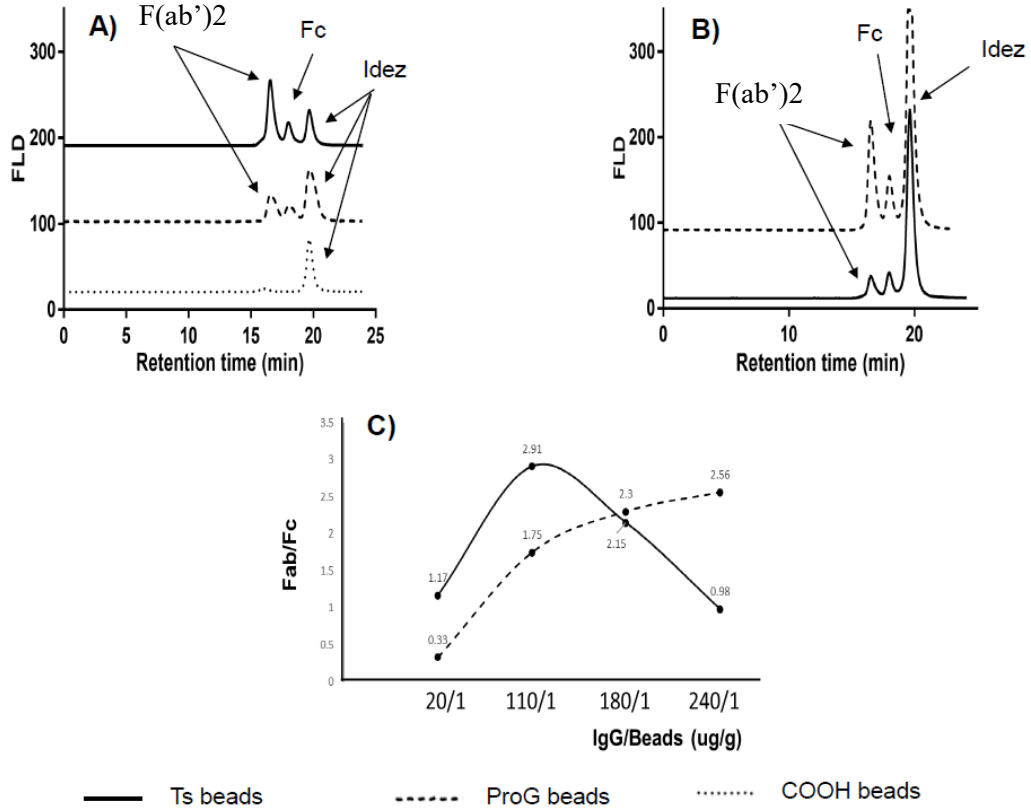
442 Fig. 4. Digestion of NAB228 antibodies (0.1 mg/ml IgG2a) in PBS by IdeZ under different  
443 digestion conditions. SEC-FLD conditions as in Fig. 3



— Optimized digested IgG  
- - - Initial digested IgG  
..... Native IgG

444  
445  
446  
447  
448  
449  
450  
451  
452  
453  
454  
455  
456  
457

458 Fig. 5. Digestion of NAB228 antibodies grafted on different magnetic beads (*i.e.*,  
459 carboxylated, tosylactivated, protein G using IgG/ beads ( $\mu\text{g}/\text{mg}$ ) ratio of A) 110:  
460 1; B) 240:1. C) Dependence of  $\text{F(ab}'_2) : \text{Fc}$  peak ratios on IgG quantity for on-bead  
461 grafting. SEC-FLD conditions as in Fig. 3



462

463

464

465

466

467

468

469

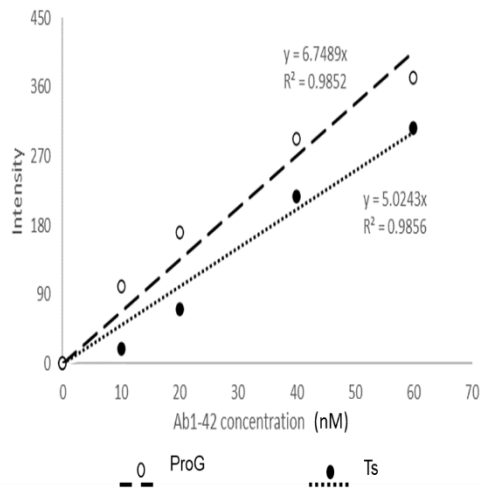
470

471 Fig. 6. A) Schematic of the immunoassay with fluorescent detection of Ab1-42 on different  
472 magnetic beads grafted with NAB288. Detection was carried out using ELISA with  
473 12F4 HRP as the detection antibody. See section 2.3 for ELISA protocol. B)  
474 Calibration curves for Ab1-42 made with NAB288 grafted on ProG and  
475 Tosylactivated beads

476 A)



479 B)



487

488 **References:**

489 [1] C. Comanescu, Magnetic Nanoparticles: Current Advances in Nanomedicine, Drug

490 Delivery and MRI, Chemistry-Switzerland 4(3) (2022) 872-930.

491 [2] C. Susy Piovesana and Anna Laura, Magnetic Materials for the Selective Analysis of

492 Peptide and Protein Biomarkers, Curr. Med. Chem. 24(5) (2017) 438-453.

493 [3] S. Khizar, H. Ben Halima, N.M. Ahmad, N. Zine, A. Errachid, A. Elaissari, Magnetic

494 nanoparticles in microfluidic and sensing: From transport to detection, Electrophoresis

495 41(13-14) (2020) 1206-1224.

496 [4] M. Serra, D. Ferraro, I. Pereiro, J.L. Viovy, S. Descroix, The power of solid supports in

497 multiphase and droplet-based microfluidics: towards clinical applications, Lab on a

498 Chip 17(23) (2017) 3979-3999.

499 [5] T.D. Mai, D. Ferraro, N. Aboud, R. Renault, M. Serra, N.T. Tran, J.-L. Viovy, C. Smadja,

500 S. Descroix, M. Taverna, Single-step immunoassays and microfluidic droplet operation:

501 Towards a versatile approach for detection of amyloid- $\beta$  peptide-based biomarkers of

502 Alzheimer's disease, Sens. Actuators B 255 (2018) 2126-2135.

503 [6] B. Moreira-Alvarez, L. Cid-Barrio, H.S. Ferreira, J.M. Costa-Fernández, J. Encinar,

504 Integrated analytical platforms for the comprehensive characterization of bioconjugated

505 inorganic nanomaterials aiming at biological applications, Journal of Analytical Atomic

506 Spectrometry 35 (2020) 1518-1529.

507 [7] S.Y. Liu, E. Haller, J. Horak, M. Brandstetter, T. Henser, M. Lamerhofer, Protein A- and

508 Protein G-gold nanoparticle bioconjugates as nano-immunoaffinity platform for human

509 IgG depletion in plasma and antibody extraction from cell culture supernatant, Talanta

510 194 (2019) 664-672.

- 511 [8] D. Bouzas-Ramos, L. Trapiella-Alfonso, K. Pons, J.R. Encinar, J.M. Costa-Fernández, V.  
512 Tsatsaris, N. Gagey-Eilstein, Controlling Ligand Surface Density on Streptavidin-  
513 Magnetic Particles by a Simple, Rapid, and Reliable Chemiluminescent Test,  
514 *Bioconjugate Chem.* 29(8) (2018) 2646-2653.
- 515 [9] R. Kozłowski, A. Ragupathi, R.B. Dyer, Characterizing the Surface Coverage of Protein-  
516 Gold Nanoparticle Bioconjugates, *Bioconjug. Chem.* 29(8) (2018) 2691-2700.
- 517 [10] C.D. Walkey, J.B. Olsen, H. Guo, A. Emili, W.C.W. Chan, Nanoparticle Size and  
518 Surface Chemistry Determine Serum Protein Adsorption and Macrophage Uptake,  
519 *JACS* 134(4) (2012) 2139-2147.
- 520 [11] H. Hinterwirth, W. Lindner, M. Lämmerhofer, Bioconjugation of trypsin onto gold  
521 nanoparticles: Effect of surface chemistry on bioactivity, *Anal. Chim. Acta* 733 (2012)  
522 90-97.
- 523 [12] Y.M. Bae, B.-K. Oh, W. Lee, W.H. Lee, J.-W. Choi, Study on orientation of  
524 immunoglobulin G on protein G layer, *Biosens. Bioelectron.* 21(1) (2005) 103-110.
- 525 [13] H.Y. Song, X. Zhou, J. Hobley, X. Su, Comparative Study of Random and Oriented  
526 Antibody Immobilization as Measured by Dual Polarization Interferometry and Surface  
527 Plasmon Resonance Spectroscopy, *Langmuir* 28(1) (2012) 997-1004.
- 528 [14] K. Yoshimoto, M. Nishio, H. Sugasawa, Y. Nagasaki, Direct Observation of Adsorption-  
529 Induced Inactivation of Antibody Fragments Surrounded by Mixed-PEG Layer on a  
530 Gold Surface, *JACS* 132(23) (2010) 7982-7989.
- 531 [15] K. Fujiwara, H. Watarai, H. Itoh, E. Nakahama, N. Ogawa, Measurement of antibody  
532 binding to protein immobilized on gold nanoparticles by localized surface plasmon  
533 spectroscopy, *Anal. Bioanal. Chem.* 386(3) (2006) 639-644.

- 534 [16] L. Zhang, D. Hu, M. Salmain, B. Liedberg, S. Boujday, Direct quantification of surface  
535 coverage of antibody in IgG-Gold nanoparticles conjugates, *Talanta* 204 (2019) 875-  
536 881.
- 537 [17] T. Näreoja, A. Ebner, H.J. Gruber, B. Taskinen, F. Kienberger, P.E. Hänninen, V.P.  
538 Hytönen, P. Hinterdorfer, H. Härmä, Kinetics of bioconjugate nanoparticle label  
539 binding in a sandwich-type immunoassay, *Anal. Bioanal. Chem.* 406(2) (2014) 493-  
540 503.
- 541 [18] R. Oliverio, B. Liberelle, F. Murschel, A. Garcia-Ac, X. Banquy, G. De Crescenzo,  
542 Versatile and High-Throughput Strategy for the Quantification of Proteins Bound to  
543 Nanoparticles, *ACS Applied Nano Materials* 3(10) (2020) 10497-10507.
- 544 [19] S.Y. Liu, J. Horak, M. Holdrich, M. Lammerhofer, Accurate and reliable quantification  
545 of the protein surface coverage on protein-functionalized nanoparticles, *Anal. Chim.*  
546 *Acta* 989 (2017) 29-37.
- 547 [20] M. Shen, D. Jiang, P.I.T. De Silva, B. Song, J.F. Rusling, Restricted Proteolysis and LC-  
548 MS/MS To Evaluate the Orientation of Surface-Immobilized Antibodies, *Anal. Chem.*  
549 DOI: 10.1021/acs.analchem.9b01155 (2019).
- 550 [21] E. Laborie, V. Le-Minh, T.D. Mai, M. Ammar, M. Taverna, C. Smadja, Analytical  
551 methods of antibody surface coverage and orientation on bio-functionalized magnetic  
552 beads: application to immunocapture of TNF- $\alpha$ , *Anal. Bioanal. Chem.* 413(25) (2021)  
553 6425-6434.
- 554 [22] N. Van Thanh Nguyen, M. Taverna, C. Smadja, T.D. Mai, Recent Electrokinetic and  
555 Microfluidic Strategies for Detection of Amyloid Beta Peptide Biomarkers: Towards  
556 Molecular Diagnosis of Alzheimer's Disease, *Chem. Record* 21(1) (2021) 149-161.

557 [23] B.L. Duivelshof, S. Fekete, D. Guillarme, V. D'Atri, A generic workflow for the  
558 characterization of therapeutic monoclonal antibodies—application to daratumumab,  
559 Anal. Bioanal. Chem. 411(19) (2019) 4615-4627.  
560